

# Comparison of different radionuclide dating models for estimating the ages of sediments from Lakes Shinji-ko and Nakaumi, Japan

Ritsuo Nomura<sup>1</sup> and Mutsuo Inoue<sup>2</sup>

**Abstract:** Understanding the history and processes of sediment accumulation in lakes and estuaries is fundamental for evaluating environmental changes in water bodies. This study presents the spatial distribution of excess  $^{210}\text{Pb}$  ( $^{210}\text{Pb}_{\text{ex}}$ ) and  $^{137}\text{Cs}$  concentrations (activities) in sediment cores from 41 sites in Lake Shinji-ko and seven sites in Lake Nakaumi, which together form the largest brackish water body in Japan. These data provide significant information on sediment age, essential for paleoenvironmental research and lake conservation.  $^{210}\text{Pb}_{\text{ex}}$  and  $^{137}\text{Cs}$  can provide very effective estimates of sediment ages over the past 100 years; however, their improper use or interpretation may result in incorrect age estimates. We review this problem by comparing various dating models, using data collected from the two lakes and evaluating their potential for sediment dating. The key requirement for accurate sediment dating is to examine the depth distribution of  $^{210}\text{Pb}_{\text{ex}}$  before selecting the dating model. Additional recommendations for the effective dating of sediments are provided.

**Key words:** Sediment dating,  $^{210}\text{Pb}$ ,  $^{137}\text{Cs}$ , Dating models, Shinji-ko, Nakaumi

## Introduction

Bottom sediments in lakes and estuaries are useful for evaluating environmental changes in water bodies. A fundamental prerequisite for such studies is an understanding of the sediment accumulation history and sedimentary processes. Atmospheric  $^{210}\text{Pb}$  (half-life = 22.3 years) has often been used in sedimentation research in various environments. Since Goldberg

(1963) developed a  $^{210}\text{Pb}$  decay model for glaciers, and Krishnaswamy et al. (1971) and Koide et al. (1972) applied this method to lake and marine varve sediments, respectively, many researchers have recognized the importance of sediment dating using  $^{210}\text{Pb}$ . Due to its half-life,  $^{210}\text{Pb}$  is a useful tracer of sedimentation histories spanning the last 120–150 years (e.g., Swarzenski, 2014). The artificial  $^{137}\text{Cs}$  (half-life = 30.2 years) is another good tracer, because large amounts of this isotope were

<sup>1</sup> Geological Laboratory, Faculty of Education, Shimane University, Matsue, Shimane Prefecture, 690-8504, Japan.

<sup>2</sup> Low Level Radioactivity Laboratory, Kanazawa University, Wake, Nomi, Ishikawa Prefecture, 923-1224, Japan.

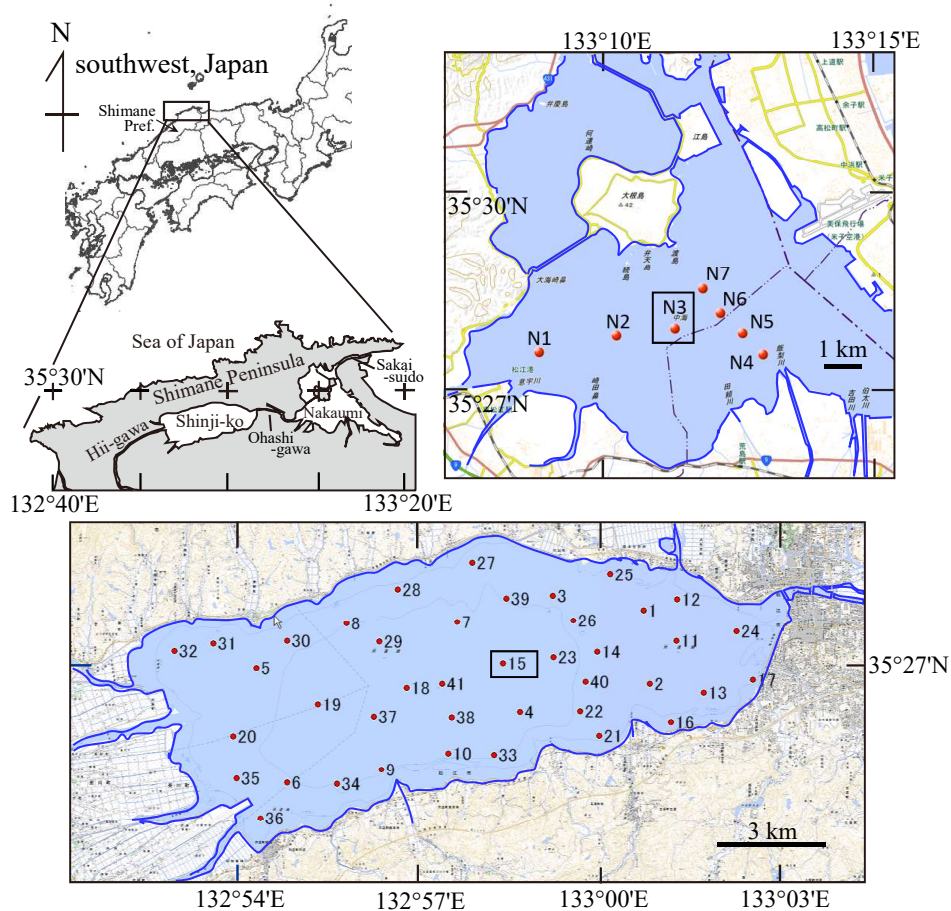


**Fig. 1** Sampling sites in Lakes Shinji-ko and Nakaumi.  $^{210}\text{Pb}$  geochronology sites are indicated by squares.

released into the environment during atmospheric nuclear tests conducted in the 1950s and early 1960s (particularly in 1963), and during the Chernobyl reactor accident in 1986 (e.g., Cambray et al., 1976; Andersen, 2017).

Regarding dating techniques, conceptual models such as the constant initial concentration (CIC; Robbins, 1978) and the constant rate of supply (CRS; Robbins, 1978; Appleby and Oldfield, 1978) have traditionally been used by researchers (e.g., Oldfield and Appleby, 1984; Carroll and Lerche, 2003; Sanchez-Cabeza and Ruiz-Fernández, 2012). The reliability and effectiveness of dating estimates generated by these models strongly depend on the depositional processes of sediments and are often influenced by model adaptability. Thus, their applications to geochronology and sedimentology are still under debate (Carroll and Lerche, 2003; Abril, 2015).

The  $^{210}\text{Pb}$  decay model was first applied to the sedimentation rate in Lake Shinji-ko by Matsumoto (1975) at four sites. Kanai et al. (1998) increased the

number of study sites in Shinji-ko. They also conducted similar research in Lake Nakaumi and included  $^{137}\text{Cs}$  concentrations (Kanai et al., 2002). Based on these dating informations, research projects using dated sediments cores from Lakes Shinji-ko and Nakaumi have expanded into a range of fields, such as water pollution (Sugiura, 1992; Matsunaga et al., 2001; Chanrajith et al., 2001), ecology (Kusunoki et al., 2012), and environmental change (Nomura, 2003; Yamamuro et al., 2005). In this report, data on  $^{210}\text{Pb}$  and  $^{137}\text{Cs}$  concentrations collected from Lakes Shinji-ko and Nakaumi are presented for future research. In addition, the data from these two sites were used to determine the effectiveness of major data models for sediment dating.

## Study area and methods

### Lake Shinji-ko and Lake Nakaumi study areas

The lakes Shinji-ko and Nakaumi are located in eastern

Shimane Prefecture, southwestern Japan (Fig. 1). The respective areas of Lakes Shinji-ko and Nakaumi are 79.1 km<sup>2</sup> and 86.2 km<sup>2</sup>, with average water depths of 4.5 m and 5.4 m and maximum depths of 6.0 m and 8.4 m. Both lakes were formed as downstream water bodies of the Hii-gawa River. They are both brackish lakes connected by the Ohashi-gawa River, and Lake Nakaumi is also connected to the Sea of Japan through the Sakai-suido Channel. Thus, salinity of the water ranges from oligohaline to polyhaline, depending on the inflow of freshwater from the Hii-gawa River and seawater from the Sea of Japan. Salinities of surface and deep waters are 1–5 psu and 5–10 psu, respectively, in Lake Shinji-ko, and 10–20 psu and 30 psu in Lake Nakaumi (Izumo Work Office, Ministry of Land, Infrastructure and Transport of Japan, 2019). In both lakes, the bottom sediments below 3.5 m water depth are composed of silt and clay, whereas those in less than 2.0 m depth are mostly sand (Mitsunashi and Tokuoka, 1988).

### Core sites and sediment sampling

The core sampling sites in Shinji-ko and Nakaumi are presented in Fig. 1 and Appendix 1. We collected sediment cores at 41 sites in water depths of 1.0–5.6 m from Lake Shinji-ko from April 2011 to July 2016, and at seven sites in water depths of 4.5–6.8 m from Nakaumi from April to December 2016. All sediment cores were taken using a push-in device with a 1-m-long acrylic pipe with a diameter of 6 cm. Cores measuring ~50–80 cm in length were carefully extracted, avoiding any physical damage. Core samples were typically collected at 2–5 sites each day. After the cores were sampled, they were sliced into sections within one or two days to avoid shrinking and chemical decomposition of the sediment. Each sediment core was cut into sections of 0.5 or 1.0-cm thickness by extruding up the sediment. Each core section was then divided into two parts. After measuring the wet weights of both parts, one part was washed through a sieve with a mesh size of 75 μm for microfossil analysis and the other one was dried to measure the water content, and subsequently powdered for γ-spectrometry.

### γ-spectrometry

Powdered sediment samples of 2 g each were sealed in a sample tube for approximately three weeks to reach equilibrium between <sup>226</sup>Ra and its <sup>222</sup>Rn granddaughters.

Subsequently, γ-spectrometry was performed on all sediment samples using two well-type Ge-detectors—an EGPC 150-P16 (Canberra-Eurysis) and a Broad Energy (BE) spectrometer, GX4019 (Canberra)—for 20 counting hours. The detection characteristics of the former are as follows; full width at half maximum (FWHM) 1.95 keV for <sup>60</sup>Co at 1332 keV, peak to Compton 58, and relative efficiency 37.9 %. The detection characteristics of the latter instrument are as follows; FWHM 1.73 keV for <sup>60</sup>Co at 1332 keV, peak to Compton 72, and relative efficiency 42.8%.

As the measured value of <sup>210</sup>Pb (46 keV) is composed of both supported and unsupported <sup>210</sup>Pb, the supported <sup>210</sup>Pb is ascribed to production from the parent <sup>226</sup>Ra in sediment. Therefore, the supported <sup>210</sup>Pb concentration, calculated from the γ-peaks of <sup>214</sup>Pb (295 and 352 keV), was subtracted from the total <sup>210</sup>Pb concentration to obtain the unsupported (i.e., excess) <sup>210</sup>Pb (<sup>210</sup>Pb<sub>ex</sub>, hereafter) concentration. <sup>210</sup>Pb, <sup>226</sup>Ra, and <sup>137</sup>Cs (662 keV) concentrations in sediment samples were calibrated using a standard material, New Brunswick Laboratory (NBL), USA, CMS 42A-2.

### Core depth and Inventory

There are two criteria for deposit thickness and weight when analyzing sediment samples in relation to time; the core depth, expressed as the sedimentation rate (cm/year), and the mass depth, expressed as the mass accumulation rate (g/cm<sup>2</sup>/year). The mass depth *m* (g/cm<sup>2</sup>) is calculated as follows:

$$m = \sum_{i=1}^n x_i \rho_{ds}$$

where *x<sub>i</sub>* is the thickness of the *i*-th core section (cm) and (*ρ<sub>ds</sub>* is the bulk density of the sectioned sediment. The bulk density (*ρ<sub>ds</sub>*: g/cm<sup>3</sup>) is given by the following formula introduced by Walling et al. (2002):

$$\rho_{ds} = \frac{\rho_s f}{f + (1 - f) \cdot \rho_w / \rho_w}$$

where *f* is the dry-weight fraction of sectioned sediment, i.e. the ratio of dry mass to wet mass, *ρ<sub>s</sub>* is the solid density, which is typically *ρ<sub>s</sub>* = ~2.5, and *ρ<sub>w</sub>* is the density of water (1 g/cm<sup>3</sup>).

The core depth is the cumulative length of sectioned core sediments under compression. The corrected core

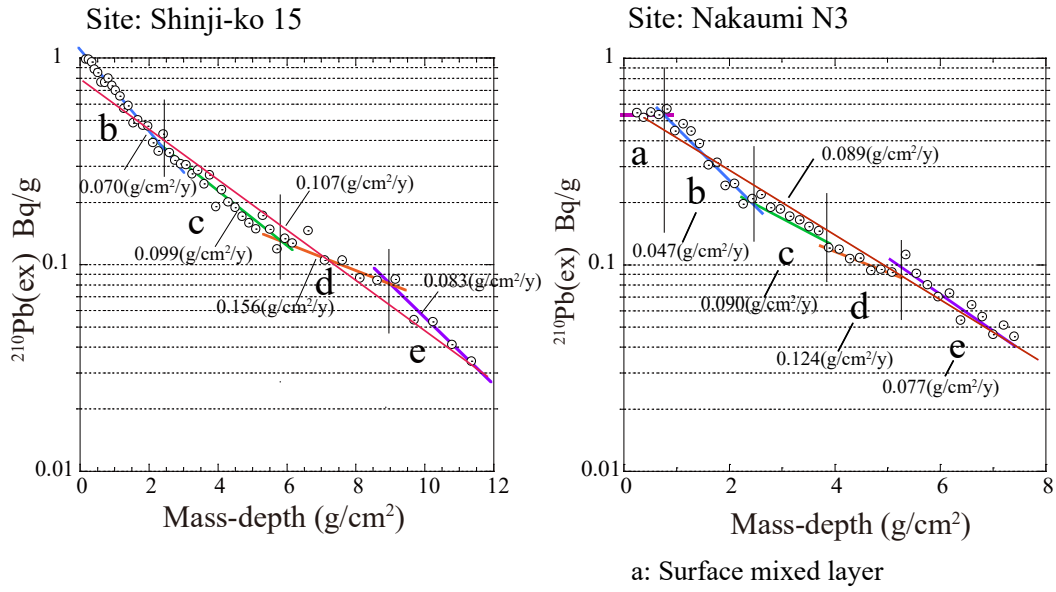


**Fig. 2** Piecewise linear analyses showing the sediment accumulation rate in the CFCS model at sites Shinji-ko-15 and Nakaumi-N3.

depth is the length of the sediment without compression ( $x'$ ), which is calculated as follows:

$$\Delta = (\phi_0 - \phi)/(1 - \phi_0),$$

$$x' = x + \sum_{i=1}^n \Delta_i$$

where  $\phi_0$  and  $\phi$  are the porosities of sediments at the topmost core section and at depth  $x$ , respectively.  $\Delta$  is the compression difference for the sediment and  $\Delta_i$  is that of the  $i$ -th core section (Matsumoto, 1975).

The inventory ( $I$ ) is calculated as follows:

$$I = \sum_{i=1}^n x_i (1 - \phi_i) \rho_s A_i$$

where  $x_i$  is the thickness of the  $i$ -th core section,  $\phi_i$  is the water content,  $\rho_s$  is the solid density, and  $A_i$  is the  $i$ -th  $^{210}\text{Pb}_{\text{ex}}$  or  $^{137}\text{Cs}$  concentration.

### Dating models

In this study, we examined the following six dating models that have been proposed to date: the CIC, CFCS, CRS, composite CRS with time marker, SIT, and the TERESA (definitions of abbreviations are shown below). In addition to these models, we referred to the Excel-based program provided by Binford (1990) and Sanchez-Cabeza and Ruiz-Fernández (2012).

(1) The Constant Initial Concentration (CIC) model is as follows:

$$C_i = C_0 e^{-\lambda t},$$

$$t = \frac{1}{\lambda} \ln \left( \frac{C_0}{C_i} \right)$$

where  $C_0$  is the  $^{210}\text{Pb}_{\text{ex}}$  concentration in the surface sediment and  $C_i$  is the concentration in the  $i$ -th core section.  $\lambda$  is the  $^{210}\text{Pb}$  decay-constant and  $t$  is the age of the sediment. This model, which assumes a variable sedimentation rate and constant initial  $^{210}\text{Pb}_{\text{ex}}$  concentration with time, is also widely known as the Constant Specific Activity (CSA) or Constant Activity (CA) model (e.g., Appleby and Oldfield, 1978; Robbins, 1978; Sanchez-Cabeza and Ruiz-Fernández, 2012). The age uncertainty was calculated using the formula of Sanchez-Cabeza and Ruiz-Fernández (2012). This model is strongly influenced by the initial  $^{210}\text{Pb}_{\text{ex}}$  concentration estimate, i.e. the concentration at zero year. We determined the initial concentration from the slope that showed a high correlation between  $^{210}\text{Pb}_{\text{ex}}$  concentration vs. depth plot in the upper several cm of sediment, excluding those layers that indicated sediment mixing.

(2) The Constant Flux Constant Sedimentation (CFCS) model was first presented by Krishnaswami et al.

(1971) and is known as a simple model (Robins, 1978). Matsumoto (1975) previously used this model for  $^{210}\text{Pb}_{\text{ex}}$  concentrations in the sediments in Lake Shinji-ko. This model is as follows:

$$C_i = C_0 e^{-\lambda m_i/r},$$

$$C_0 = F/r$$

where  $F$  is the  $^{210}\text{Pb}_{\text{ex}}$  flux ( $\text{Bq}/\text{cm}^2/\text{year}$ ) and  $r$  is the mass accumulation rate ( $\text{g}/\text{cm}^2/\text{year}$ ). The sedimentation rate is determined from the mean slope by exponential linear fitting of the  $^{210}\text{Pb}_{\text{ex}}$  concentration vs. depth plot. However, because changes in flux may occur, a piecewise-linear approach is used to determine if intervals with differing sedimentation rates exist. At site Shinji-ko-15, for example, four different piecewise-linear segments were defined, in which high regression coefficients were exhibited. At Nakaumi-N3, five intervals with different regression lines were observed. Of these, the upper 2 cm exhibited notably lower concentrations of  $^{210}\text{Pb}_{\text{ex}}$  (Fig. 2), which has often been observed in previous studies of  $^{210}\text{Pb}$  geochronology (Koide et al., 1973; Robbins and Edginton, 1975; Oguri et al., 2003). According to Robbins and Edginton (1975), Osaki et al. (1997), and Dellapenna et al. (1998), this may be due to post-depositional redistribution of the sediment, possibly caused by bioturbation and/or physical mixing at the sediment-water interface. In the case of organic rich sediments such as peat,  $^{210}\text{Pb}$  is immobile (MacKenzie et al., 1997; Vile et al., 1999), and the diffusional mobility of total  $^{210}\text{Pb}$  results from redox conditions occurring in pore water (Nittrouer, et al., 1984; Binford et al., 1993; von Gunten and Moser, 1993; Hancock et al., 2002). Consequently, we exclude this sediment interval from dating. Lastly, the age uncertainty is determined by using the formula of Sanchez-Cabeza and Ruiz-Fernández (2012).

(3) The Constant Rate of Supply (CRS) model is presented by the following formulae:

$$A_{(i)} = A_{(0)} e^{-\lambda t},$$

$$t = \frac{1}{\lambda} \ln \left( \frac{A_{(0)}}{A_{(i)}} \right)$$

where  $A_{(0)}$  is the total inventory of  $^{210}\text{Pb}_{\text{ex}}$  in the sediment column and  $A_{(i)}$  is the cumulative inventory according to the sediment depth of the  $i$ -th core section. This

model, which assumes a constant flux of  $^{210}\text{Pb}_{\text{ex}}$  to the sediments and variable sedimentation rates, is most widely used in  $^{210}\text{Pb}$  geochronology and is sometimes also referred to as the constant flux (CF) model (Appleby and Oldfield, 1978; Robbins, 1978; Sanchez-Cabeza and Ruiz-Fernández, 2012) or the constant flux lead-210 model (CFL: Lu and Matsumoto, 2005). To calculate  $A_{(0)}$ , we used the method of Appleby (2001), who applied the trapezium rule to calculate the cumulative  $^{210}\text{Pb}_{\text{ex}}$  inventories. The formula to calculate the uncertainty of age was also derived from Appleby (2001). To compare the dating results, we also used a program developed by Sanchez-Cabeza and Ruiz-Fernández (2012), which utilizes the sediment weight per core volume to calculate the bulk density.

(4) The composite model, in which the known dates in specific depths are incorporated into the CRS model, was developed by Appleby (1998; 2001). The global fallout-derived  $^{137}\text{Cs}$  concentrations from 1963 are typically applied to this model. The changes in the  $^{210}\text{Pb}_{\text{ex}}$  supply rate ( $P$ ) are calculated as follows:

$$P = \frac{\lambda \Delta A}{e^{-\lambda t_1} - e^{-\lambda t_2}}$$

where  $\Delta A$  is the  $^{210}\text{Pb}_{\text{ex}}$  inventory between depths  $x_1$  and  $x_2$ , with known dates  $t_1$  and  $t_2$ , respectively. The time between  $x_1$  and  $x_2$  is determined by the following formula:

$$t = \frac{1}{\lambda} \ln \left( \frac{P/\lambda}{P/\lambda - \hat{A}} \right)$$

where  $\hat{A}$  is the  $^{210}\text{Pb}_{\text{ex}}$  inventory between depth  $x_1$  and  $x_2$ , and the age below depth  $x_2$  is calculated as follows:

$$t = t_1 + \frac{1}{\lambda} \ln \left( 1 + \frac{A_{(i)}}{\hat{A}} \right)$$

where  $A_{(i)}$  is the cumulative inventory from depths  $x_2$  to  $x_i$  and  $\hat{A}$  is the total inventory below depth  $x_2$ .

(5) The Sediment Isotope Tomography (SIT) model (Carroll and Lerche, 2003) was developed considering that both, sediment accumulation rates and  $^{210}\text{Pb}_{\text{ex}}$  fluxes vary with time (Liu et al., 1991). It represents changes of  $^{210}\text{Pb}_{\text{ex}}$  concentration  $C(x)$  with sediment depth ( $x$ ) by the following two terms (the former is referred to as sedimentation term and the latter as source term):

$$C(x) = C_0 \cdot \exp \left[ \left( -Bz + \sum_{n=1}^N \frac{a_n}{n\pi} \sin \left( \frac{n\pi z}{x_{max}} \right) \right) + \sum_{n=1}^N \frac{b_n}{n\pi} \left( 1 - \cos \left( \frac{n\pi z}{z_{max}} \right) \right) \right],$$

where  $C_0$  is the initial  $^{210}\text{Pb}_{\text{ex}}$  concentration ( $\text{Bq}/\text{cm}^3$ );  $x_{max}$  is the greatest depth of measurement;  $B$  represents slowness (year/cm) related to the average sedimentation rate ( $v$ ),  $B=1/v$ ;  $z$  is the relative depth,  $z=x/x_{max}$ ;  $a_n$  and  $b_n$  are the best parameters of Fourier series coefficients from a  $^{210}\text{Pb}_{\text{ex}}$ -depth data set. The age ( $t$ ) is determined based on the sedimentation term as follows:

$$t = x_{max} \left[ Bz + \sum_{n=1}^N \frac{a_n}{\pi n} \sin(n\pi z) \right].$$

This method is unique in that it uses a Fourier series instead of describing the sedimentation process by applying an exponential decay model.

(6) The Time Estimates from Random Entries of Sediments and Activities (TERESA) model is based on the independent variability and approximate normal distribution of both, mass flow and initial  $^{210}\text{Pb}_{\text{ex}}$  concentrations. Consequently, a linear correlation can be applied to the  $^{210}\text{Pb}_{\text{ex}}$  fluxes and sediment accumulation rates (SAR), which allows for the use of the chronological model (Abril Hernández, 2016):

$$F_i = A_{0,i} \cdot w_i$$

where  $F_i$  is the  $^{210}\text{Pb}_{\text{ex}}$  flux,  $A_{0,i}$  is the initial concentration, and  $w_i$  is the sediment accumulation rate.

## Results and Discussion

The depositional processes of  $^{210}\text{Pb}_{\text{ex}}$  and  $^{137}\text{Cs}$  varied clearly between sites in both Shinji-ko and Nakaumi. The concentrations of these radionuclides across sediment depths (cm) and mass depths ( $\text{g}/\text{cm}^2$ ) are shown in Appendices 4-11. Four distinctive patterns were recognized among the depth profiles of  $^{210}\text{Pb}_{\text{ex}}$  concentrations. The first was observed at site Shinji-ko-15, where  $^{210}\text{Pb}_{\text{ex}}$  concentrations decreased exponentially with core depth (Appendix 6). The second pattern is more common and was observed at many sites, where  $^{210}\text{Pb}_{\text{ex}}$  concentrations also decreased following an

exponential function, but the curve showed breakpoints at several depth intervals; e.g., sites Shinji-ko -3, -5, -6 (Appendix 4), -7, -8, -10 (Appendix 5), -19, -23 (Appendix 7), -30 (Appendix 8), -34, -35 (Appendix 9), -37, -39 (Appendix 10), at site Nakaumi N2 (Appendix 11). The third pattern was found at sites Shinji-ko-13 (Appendix 6), -21 (Appendix 7), -27, -30 (Appendix 8), and -32, -36 (Appendix 9). At these sites,  $^{210}\text{Pb}_{\text{ex}}$  concentrations remained approximately constant over several cm of the top sediment layer. Contrarily, no regular pattern was observed at site Shinji-ko-16 (Appendix 6). Of these four observed patterns, the first three correspond to the A, B, and C types described by Goldberg and Koide (1962), who examined the depth profiles of ionium/thorium ratios in deep-sea sediments.

In addition to our findings on  $^{210}\text{Pb}_{\text{ex}}$ , a clear peak in concentrations of  $^{137}\text{Cs}$  was typically observed at various depths at each site. No clear patterns could be observed for both, however,  $^{210}\text{Pb}$  and  $^{137}\text{Cs}$  in cores from shallower depths of less than approximately 3.7 m. This can be explained by higher  $^{210}\text{Pb}$  and  $^{137}\text{Cs}$  concentrations in mud-dominated sediments (Andersen, 2017) that occurred only at greater depths at our study sites.

The geographic distributions of the  $^{210}\text{Pb}_{\text{ex}}$  inventories and  $^{137}\text{Cs}$  peak depth in the cores from Lake Shinji-ko are presented in Fig. 3. The inventories of  $^{210}\text{Pb}_{\text{ex}}$  were  $< 1\text{--}6 \text{ Bq}/\text{cm}^2$  and exhibited higher values on the west side of the lake, particularly near the mouth of the Hii-gawa River, and lower values in the east (Fig. 3a). Depth distribution of  $^{137}\text{Cs}$  peak concentrations showed a similar pattern, ranging from  $< 1$  to  $\sim 30$  cm depth (Fig. 3b). Similar distributions in Shinji-ko were described by Kanai et al. (1998). The higher inventories near the river mouth suggest that the deposition of  $^{210}\text{Pb}$  and  $^{137}\text{Cs}$  is increased by the Hii-gawa River.

To compare the results from the six different dating models, we took two representative cores from Lakes Shinji-ko (site 15) and Nakaumi (site N3) as examples. The differences between estimated age and mass depth in the CIC (CA), CFCS, CRS (CF), composite CRS, SIT, and TERESA models are shown in Fig. 4 and Appendices 2 and 3. The CRS model, which includes the CF model of Sanchez-Cabeza and Ruiz-Fernández (2012), substantially underestimated sediment age for lower mass depths and overestimated it for high mass depth values (Fig 4). This issue has previously been

Comparison of different radionuclide dating models for estimating the ages of sediments from Lakes Shinji-ko and Nakaumi, Japan

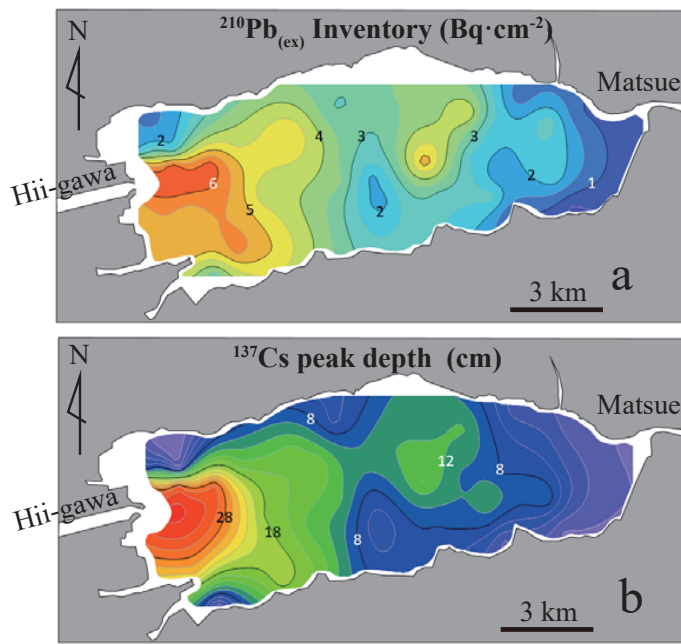


**Fig. 3**  $^{210}\text{Pb}_{\text{ex}}$  inventories showing differences in the east and west of Shinji-ko and depth distribution of  $^{137}\text{Cs}$  peaks occurring in the cores. a.  $^{210}\text{Pb}_{\text{ex}}$  inventory ( $\text{Bq}/\text{cm}^2$ ); b. Peak depth (cm) of  $^{137}\text{Cs}$ .

reported as a weakness of the CRS model (Binford, 1990; Turner and Delorme, 1996; Tylmann et al., 2013). This is ascribed to underestimation of the total inventory and could be improved by adjusting the detection limit of  $^{210}\text{Pb}_{\text{ex}}$  concentrations at greater core depths using a low background detector (MacKenzie et al., 2011). The other models (CIC, CFCS (the piecewise method), composite CRS, SIT, and TERESA) generated similar age estimates, at least for low to medium mass depths. Their differences remained within 10 years for the upper two-third of the Shinji-ko core and within 11 years for the upper half of the Nakaumi core. However, variation across models increased at greater depths.

We observed a pronounced peak of  $^{137}\text{Cs}$  at a core depth of 14.0–14.5 cm at site Shinji-ko-15 (Appendix 3) and 7.5–8.5 cm at site Nakaumi-N3 (Appendix 8). Significant fallout of artificial radionuclides, such as  $^{137}\text{Cs}$  and  $^{90}\text{Sr}$ , was observed in rain and the atmosphere in 1963–1964 across Europe, the Arctic (Cambray et al., 1976; Wright et al., 1999), and Japan (Katsuragi, 1983; Aoyama, 2006). These radionuclide concentration peaks in sediment cores are well reflected by the 1963 time marker. The composite CRS model, using the 1963 time marker, significantly underestimated sediment ages until the depth of the 1963 time marker, after that the estimation

error gradually decreased with depth. Using the sediment accumulation rates estimated by the piecewise linear regression (in this case, the upper depth distribution of  $^{210}\text{Pb}_{\text{ex}}$ ), the TERESA model was in close agreement with the 1963 time marker. However, it should be noted that the accurate estimation of sediment accumulation rates is critical and greatly affects the dating results of this model. The results of the CFCS model using piecewise linear analysis were also in agreement with the 1963 time marker at both sites. This model represented by one regression fitting of the  $^{210}\text{Pb}_{\text{ex}}$  concentration-depth relationship, however, resulted in significant differences in age estimates (Fig. 2; Appendices 2 and 3). Although the SIT model requires relatively complex calculations to determine the best parameter for the Fourier series, it produced a smooth curve for the age-depth relationship without producing unacceptable outliers for age estimation (Fig. 4). Based on these results, it is evident that sediment dating using a single model is undesirable and that a comparison of multiple calculation models is extremely important, as pointed out previously (e.g., Oldfield and Appleby, 1984; Appleby, 1998; Tylmann et al., 2016; Córdoba, et al., 2017; Andersen, 2017). We recognized that the  $^{210}\text{Pb}$  dating method is more effective when an additional, independent time marker such as

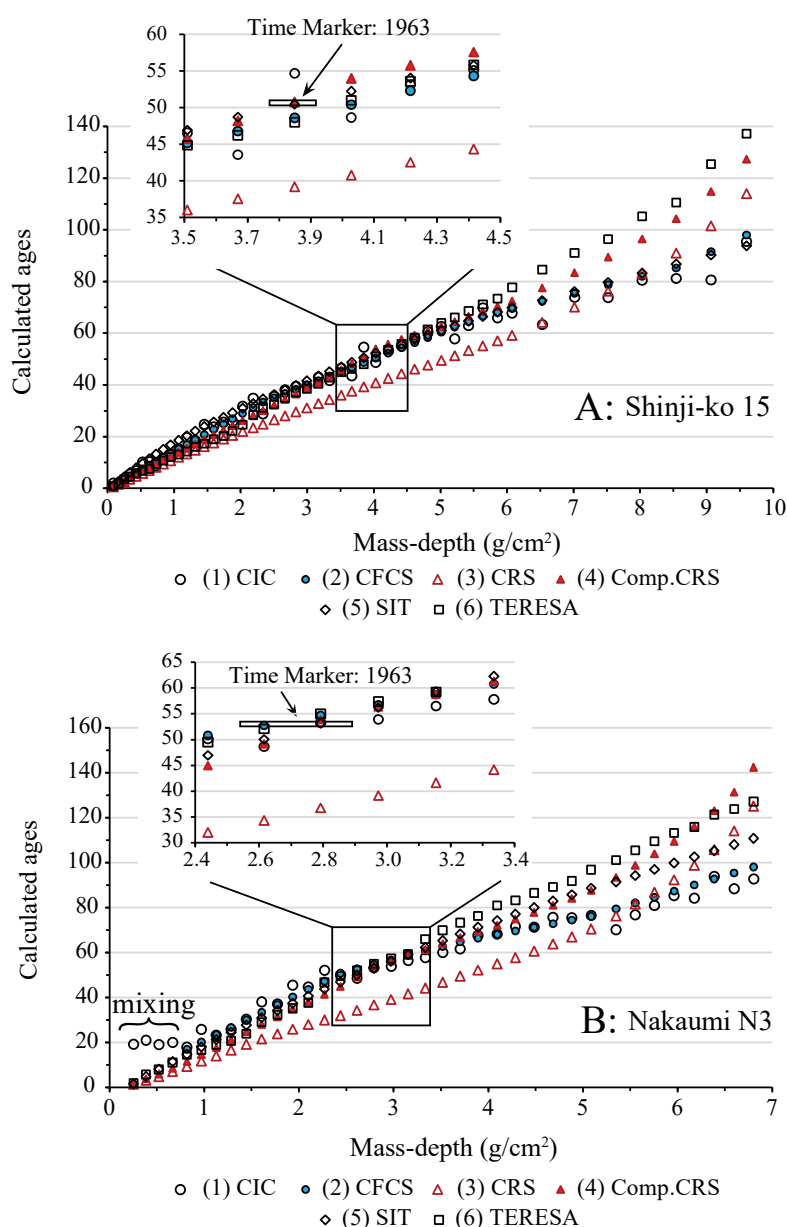


**Fig. 4** Geochronological comparison of major dating models: (1) CIC (Constant Initial Concentration), (2) piecewise CFCS (Constant Flux Constant Sedimentation), (3) CRS (Constant Rate of Supply), (4) composite CRS, (5) SIT (Sediment Isotope Tomography), and (6) TERESA (Time Estimates from Random Entries of Sediments and Activities).

$^{137}\text{Cs}$  (Kirchner and Ehlers, 1998; Miguel et al., 2003; Abril, 2004; Kirchner, 2011; Putyrskaya et al., 2015) is accurately determined in the sediment core, although a post-depositional immobility of  $^{137}\text{Cs}$  is a prerequisite for reliable sediment dating. A peak of  $^{137}\text{Cs}$  concentration was clearly detected for cores that were sliced into 0.5-cm and 1.0-cm thickness (particularly 0.5-cm thickness) in most Shinji-ko and Nakaumi cores. On the other hand,  $^{137}\text{Cs}$  concentration peaks were not well defined in some

cores, for example at sites Shinji-ko-3, -7, -30, and -40 (Appendix 4, 5, 8, 10), showing the masses of several higher peaks instead. These vertical distributions of  $^{137}\text{Cs}$  concentration are predominantly reflecting the difference of sedimentation rate at each site. It is considered that finer resolution analysis is required to evaluate how to determine the core depth of time markers and to decrease the uncertainty for sediment dating if multiple or broad peaks of  $^{137}\text{Cs}$  concentration are present. If we refer to



the composite CRS model at Shinji-ko-15 for example, a 1-cm core thickness (14.75-13.75 cm in depth) resulted in about 5.8-years uncertainty (Appendix 2). Sediment dating using unreliable peak position may limit the effectiveness of  $^{137}\text{Cs}$  as a time marker.

### Recommendations for the effective dating

Any dating model based on assumptions, such as a constant sedimentation rate or radionuclide flux, will generate uncertainties. Consequently, reliable dating techniques require incorporating the characteristics of each model effectively. Comprehensive reviews on procedures and analyses for dating estuarine and marine sediments have recently been provided by Swarzenski (2014) and Andersen (2017). Whereas sediment cores with higher sedimentation rates ( $> \sim 0.3$  cm/year) can be sectioned into 1-cm thickness, it is recommendable to use 0.5-cm thickness for samples with lower sedimentation rates ( $< \sim 0.2$  cm/year). Detailed examinations of the depth distribution of  $^{210}\text{Pb}_{\text{ex}}$  concentrations are required for selecting the dating model and accurate sediment dating.

All data of  $^{210}\text{Pb}$  and  $^{137}\text{Cs}$  sediment concentration from Shinji-ko and Nakaumi can be found at the following website: [http://www.jaes.shimane-u.ac.jp/?page\\_id=31](http://www.jaes.shimane-u.ac.jp/?page_id=31). Sediment samples stocked in the Estuary Center of Shimane University can be provided upon researcher's request.

### Acknowledgements

We would like to thank Dr. Akira Tsujimoto, Shimane University, for his assistance. Dr. Abril Hernandez, J.-M., Spain, provided instructive comments on the TERESA model. This work was supported by a Japanese Grant-in Aid for Scientific Research (B) (R. Nomura, Nos. 21340147, 25287138) and (C) (R. Nomura, No. 17K02110).

### References

Abril, J.M. (2004) Constraints on the use of  $^{137}\text{Cs}$  as a time-marker to support CRS and SIT chronologies. *Environmental Pollution*, 129: 31–37.  
Abril, J.M. (2015) Why would we use the sediment

isotope tomography (SIT) model to establish a  $^{210}\text{Pb}$ -based chronology in recent-sediment cores? *Journal of Environmental Radioactivity*, 143: 40–46.  
Abril Hernández J.M. (2016) A  $^{210}\text{Pb}$ -based chronological model for recent sediments with radon entries of mass and activities: Model development. *Journal of Environmental Radioactivity*, 151: 64–74.  
Andersen, T.J. (2017) Some practical considerations regarding the application of  $^{210}\text{Pb}$  and  $^{137}\text{Cs}$  dating to estuarine sediments. In: *Applications of Paleoenvironmental Techniques in Estuarine Studies*, (eds.) Weckström, K., Saunders, K.M., Gell, P.A. and Skilbeck, C.G. pp. 121–140. Springer, Dordrecht, The Netherlands.  
Aoyama, M. (2006) Present status and prospects of ultralow level radioactivity measurement (4). Ultralow level radioactivity measurements of fallout and deep sea samples. *Radioisotopes*, 55: 429–438. (in Japanese)  
Appleby, P.G. (1998) Dating recent sediment by  $^{210}\text{Pb}$ : Problems and solutions. In: *Dating of sediments and determination of sedimentation rate*, (ed.) Ilus, E. pp. 7-24. Proceedings of a seminar held in Helsinki, 2-3 April, 1997 (ISBN: 951-712-226-8).  
Appleby, P.G. (2001) Chronostratigraphic techniques in recent sediments. In: *Tracking Environmental Change Using Lake Sediments. Volume 1: Basin Analysis, Coring, and Chronological Techniques*, (eds.) Last, W.M. and Smol, J.P. pp. 171–203. Kluwer Academic Publ., Dordrecht, The Netherlands.  
Appleby, P.G. and Oldfield, F. (1978) The calculation of  $^{210}\text{Pb}$  dates assuming a constant rate of supply of unsupported  $^{210}\text{Pb}$  to the sediment. *Catena*, 5: 1–8.  
Binford, M.W. (1990) Calculation and uncertainty analysis of  $^{210}\text{Pb}$  dates for PIRLA project lake sediment cores. *Journal of Paleolimnology*, 3: 253–267.  
Binford, M.W., Kahl, J.S. and Norton, S.A. (1993) Interpretation of  $^{210}\text{Pb}$  profiles and verification of the CRS dating model in PIRLA project lake sediment cores. *Journal of Paleolimnology*, 9: 275–296.  
Cambray, R.S., Fisher, M.E.R., Eakins, J.D. and Peirson, D.H. (1976) Radioactive fallout in air and rain: Results to the end of 1975. UK Atomic Authority, AERE-R 8267. Harwell, Oxfordshire, 54 p.  
Carroll, J. and Lerche, I. (2003) *Sedimentary processes: Quantification using radionuclides*. Radioactivity in the Environment. Elsevier, Oxford, 272 p.

- Chandrajith, R., Okumura, M. and Ueno, T. (2001) Record of mercury pollution in sediments of lakes Nakaumi and Shinji in Japan. *Lakes & Reservoirs: Research and Management*, 6: 127–131.
- Córdoba, F.E., Piovano, E.L., Guerra, L., Mulsow, S., Sylvestre, F. and Zárate, M. (2017) Independent time markers validate  $^{210}\text{Pb}$  chronologies for two shallow Argentine lakes in Southern Pampas. *Quaternary International*, 438: 175–186.
- Dellapenna, T.M., Kuchi, S.A. and Schaffner, L.C. (1998) Sea-bed mixing and particle residence times in biologically and physically dominated estuarine system: A comparison of lower Chesapeake Bay and the York River subestuary. *Estuarine, Coastal Shelf Science*, 46: 777–795.
- Goldberg, E.D. (1963) Geochronology with  $^{210}\text{Pb}$ . In: *Radioactive Dating: Proceedings of the Symposium on Radioactive Dating held by the International Atomic Energy Agency in Co-operation with the Joint Commission on Applied Radioactivity (ICSU) in Athens, November 19-23, 1962*, pp.121–131, Athens, Greece.
- Goldberg, E.D. and Koide, M. (1962) Geochronological studies of deep sea sediments by the ionium/thorium method. *Geochimica et Cosmochimica Acta*, 26: 417–450.
- Hancock, G., Edgington, D.N., Robbins, J.A., Smith, J.N., Brunskill, G. and Pfitzer, J. (2002) Workshop on radiological techniques in sedimentation studies: Methods and applications. In: *Environmental Changes and Radioactive Tracers*, (eds.) Fernandez, J.M. and Fichez, R. pp. 233–251. 6th South Pacific Environmental Radioactivity Association Conference 19–23, June, 2000. Nouméa IRD Centre, New Caledonia.
- Izumo Work Office, Ministry of Land, Infrastructure and Transport of Japan (2019) <http://www.cgr.mlit.go.jp/izumokasen/shiryokan/jokyo/index.html>. (cited in 2019, 6, 15)
- Kanai, Y., Inouchi, Y., Yamamuro, M., and Tokuoka, T. (1998) Sedimentation rate and environment in Lake Shinji, Shimane Prefecture. *Chikyukagaku (Geochemistry)*, 32: 71–85. (in Japanese with English abstract)
- Kanai, Y., Yamamuro, M., Inouchi, Y., and Tokuoka, T. (2002) Sedimentation rate and environment of Lake Nakaumi, Shimane and Tottori Prefectures. *Chikyukagaku (Geochemistry)*, 36: 161–178. (in Japanese with English abstract)
- Katsuragi, Y. (1983) A study of  $^{90}\text{Sr}$  fallout in Japan. *Papers in Meteorology and Geophysics*, 33: 277–291.
- Kirchner, G. (2011) Pb-210 as a tool for establishing sediment chronologies: Examples of potentials and limitations of conventional dating methods. *Journal of Environmental Radioactivity*, 102: 490–494.
- Kirchner, G. and Ehlers, H. (1998) Sediment geochronology in Changing coastal environments: Potentials and limitations of the  $^{137}\text{Cs}$  and  $^{210}\text{Pb}$  methods. *Journal of Coastal Research*, 14: 483–492.
- Koide, M., Soutar, A. and Goldberg, E.D. (1972) Marine geochronology with  $^{210}\text{Pb}$ . *Earth and Planetary Science Letters*, 14: 442–446.
- Koide, M., Bruland, K.W. and Goldberg, E.D. (1973) The Th-228/Th-232 and Pb-210 geochronologies in marine and lake sediments. *Geochimica et Cosmochimica Acta*, 37: 1171–1187.
- Krishnaswamy, S., Lal, D., Martin, J.M. and Meybeck, M. (1971) Geochronology of lake sediments. *Earth and Planetary Science Letters*, 11: 407–414.
- Kusunoki, K., Sakata, M., Tani, Y., Seike, Y. and Ayukawa, K. (2012) Analysis of historical trend of carotenoid concentrations in sediment cores from Lake Shinji, Japan. *Geochemical Journal*, 46: 225–233.
- Liu, J., Carroll, J.L. and Lerche, I. (1991) A technique for disentangling temporal source and sediment variations from radioactive isotope measurements with depth. *Nuclear Geophysics*. 5: 31–45.
- Lu, X. and Matsumoto, E. (2005) Recent sedimentation rates derived from  $^{210}\text{Pb}$  and  $^{137}\text{Cs}$  methods in Ise Bay, Japan. *Estuarine, Coastal and Shelf Science*, 65: 83–93.
- MacKenzie, A.B., Hardie, S.M.L., Farmer, J.G., Eades, L.J. and Pulford, I.D. (2011) Analytical and sampling constraints in  $^{210}\text{Pb}$  dating. *Science of the Total Environment*, 409: 1298–1304.
- MacKenzie, A.B., Farmer, J.G. and Sugden, C.L. (1997) Isotopic evidence of the relative retention and mobility of lead and radiocaesium in Scottish ombrotrophic peats. *Science of the Total Environment*, 203: 115–127.
- Matsumoto, E. (1975)  $^{210}\text{Pb}$  geochronology of sediments from Lake Shinji. *Geochemical Journal*, 9: 167–172.
- Matsunaga, S., Yao, Y., Ogura, I., Nakai, S., Kanai, Y.,

- Yamamuro, M. and Nakanishi, J. (2001) Identifying sources and mass balance of dioxin pollution in Lake Shinji Basin, Japan. *Environmental Science and Technology*, 35: 1967–1973.
- Miguel, S., Bolívar, J.P. and Garcia-Tenorio, R. (2003) Mixing, sediment accumulation and focusing using  $^{210}\text{Pb}$  and  $^{137}\text{Cs}$ . *Journal of Paleolimnology*, 29: 1–11.
- Mitsunashi, T. and Tokuoka, T. (1988) Nakaumi and Shinjiko: Geomorphology, substrate and the atlas of natural history. Center for Studies of the San'in region, Shimane University, 115 p. (in Japanese)
- Nittrouer, C.A., DeMaster, D.J., McKee, B.A., Cutshall, N.H. and Larsen, I.L. (1984) The effect of sediment mixing on Pb-210 accumulation rates for the Washington continental shelf. *Marine Geology*, 54: 201–221.
- Nomura, R. (2003) Assessing the roles of artificial vs. natural impacts on brackish lake environments: Foraminiferal evidence from Lake Nakaumi, southwest Japan. *Journal of the Geological Society of Japan*, 109: 197–214.
- Oguri, K., Matsumoto, E., Yamada, M., Saito, Y. and Iseki, K. (2003) Sediment accumulation rates and budgets of depositing particles of the East China Sea. *Deep-Sea Research*, 11: 513–528.
- Oldfield, F. and Appleby, P.G. (1984) Empirical testing of  $^{210}\text{Pb}$ -dating models for lake sediments. In: *Lake Sediments and Environmental History*. (eds.) Haworth, Y. and Lund, J.W.C., pp. 93–124. Leicester University Press.
- Osaki, S., Sugihara, S., Momoshima, N. and Maeda, Y. (1997) Biodiffusion of  $^7\text{Be}$  and  $^{210}\text{Pb}$  in intertidal estuarine sediment. *Journal of Environmental Radioactivity*, 37: 55–71.
- Putyrskaya, V., Klemm, E., Röllin, S., Astner, M. and Sahli, H. (2015) Dating of sediments from four Swiss prealpine lakes with  $^{210}\text{Pb}$  determined by gamma-spectrometry: Progress and problems. *Journal of Environmental Radioactivity* 145: 78–94.
- Robbins, J.A. (1978) Geochemical and geophysical applications of radioactive lead. In: *Biogeochemistry of Lead in the Environment*. (ed.) Nriagu, J.O., pp. 285–393, Topics in Environmental Health, Vol. 1A, Amsterdam, Elsevier/North Holland.
- Robbins, J.A. and Edgington, D.N. (1975) Determination of recent sedimentation rates in Lake Michigan using Pb-210 and Cs-137. *Geochimica et Cosmochimica Acta*, 39: 285–304.
- Sanchez-Cabeza, J.A. and Ruiz-Fernández, A.C. (2012)  $^{210}\text{Pb}$  sediment radiochronology: An integrated formulation and classification of dating models. *Geochimica et Cosmochimica Acta*, 82: 183–200.
- Sugiura, K. (1992) Congener-specific PCB analyses of a sediment core of Lake Shinji, Japan. *Chemosphere*, 24: 427–432.
- Swarzenski P.W. (2014)  $^{210}\text{Pb}$  Dating. In: *Encyclopedia of Scientific Dating Methods*. (eds.) Rink W. and Thompson J., pp. 1–11, Springer, Dordrecht, The Netherlands (available at: [https://link.springer.com/referenceworkentry/10.1007/978-94-007-6326-5\\_236-1](https://link.springer.com/referenceworkentry/10.1007/978-94-007-6326-5_236-1))
- Turner, L.J. and Delorme, L.D. (1996) Assessment of  $^{210}\text{Pb}$  data from Canadian lakes using the CIC and CRS models. *Environmental Geology*, 28: 78–87.
- Tylmann, W., Bonk, A., Goslar, T., Wulf, A. and Grosjean, M. (2016) Calibrating  $^{210}\text{Pb}$  dating results with varve chronology and independent chronostratigraphic markers: Problems and implications. *Quaternary Geochronology*, 32: 1–10.
- Tylmann, W., Enters, D., Kinder, M., Moska, P., Ohlendorf, C., Poreba, G. and Zolitschka, B. (2013) Multiple dating of varved sediments from Lake Łazduny, northern Poland: Toward an improved chronology for the last 150 years. *Quaternary Geochronology*, 15: 98–107.
- Vile, M.A., Wieder, R.K. and Novák, M. (1999) Mobility of Pb in *Sphagnum*-derived peat. *Biogeochemistry*, 45: 35–52.
- von Gunten, H.R. and Moser, R.N. (1993) How reliable is the  $^{210}\text{Pb}$  dating method? Old and new results from Switzerland. *Journal of Paleolimnology*, 9: 161–178.
- Walling, D.E., He, Q. and Appleby, P.G. (2002) Conversion models for use in soil-erosion, soil-redistribution and sedimentation investigations. In: *Handbook for the Assessment of Soil Erosion and Sedimentation Using Environmental Radionuclides*. (ed.) Sapata, F., pp. 111–162. Kluwer Academic Publishers, Dordrecht, The Netherlands.
- Wright, S.M., Howard, B.J., Strand, P., Nylén, T. and Siccek, M.A.K. (1999) Prediction of  $^{137}\text{Cs}$  deposition from atmospheric nuclear weapons tests within the Arctic. *Environmental Pollution*, 104: 131–143.
- Yamamuro, M. and Kanai, Y. (2005) A 200-year record

of natural and anthropogenic changes in water quality  
from coastal lagoon sediments of Lake Shinji, Japan.  
Chemical Geology, 218: 51–61.

**Appendix 1** List of sampling sites.

Sites	Longitude	Latitude	water depth (m)	Date of sampling
<b>Shinji-ko -</b>				
1	133.0122	35.4631	4.2	2011.4.9
2	133.0140	35.4460	4.6	2011.4.9
3	132.9864	35.4663	4.7	2012.4.16
4	132.9771	35.4395	5.2	2012.4.16
5	132.9026	35.4496	4.4	2012.8.6
6	132.9113	35.4230	4.4	2012.8.6
7	132.9595	35.4603	5.2	2012.11.18
8	132.9281	35.4600	4.9	2012.11.18
9	132.9379	35.4260	5.1	2012.11.18
10	132.9569	35.4298	5.1	2012.11.18
11	133.0214	35.4559	4.3	2013.5.1
12	133.0217	35.4655	4.0	2013.5.1
13	133.0292	35.4439	3.7	2013.7.7
14	132.9991	35.4534	4.8	2013.8.3
15	132.9723	35.4507	4.8	2013.8.3
16	133.0199	35.4371	1.0	2013.11.8
17	133.0431	35.4469	2.6	2013.11.8
18	132.9450	35.4450	5.4	2013.12.15
19	132.9200	35.4412	5.3	2013.12.15
20	132.8960	35.4338	4.6	2013.12.15
21	132.9997	35.4339	3.7	2013.12.23
22	132.9941	35.4397	4.8	2013.12.23
23	132.9867	35.4521	5.3	2013.12.23
24	133.0384	35.4581	3.3	2014.6.1
25	133.0027	35.4713	3.2	2014.6.1
26	132.9922	35.4606	4.8	2014.6.1
27	132.9636	35.4741	4.0	2014.6.1
28	132.9426	35.4678	4.2	2014.8.28
29	132.9375	35.4558	5.3	2014.8.28
30	132.9113	35.4559	4.5	2014.9.16
31	132.8905	35.4552	3.4	2014.9.16
32	132.8795	35.4536	3.2	2014.9.16
33	132.9699	35.4294	5.1	2015.3.27
34	132.9253	35.4227	5.1	2015.3.27
35	132.8970	35.4239	4.4	2015.3.27
36	132.9038	35.4148	3.4	2015.8.9
37	132.9357	35.4384	5.3	2015.8.9
38	132.9579	35.4382	5.4	2015.8.9
39	132.9733	35.4657	5.0	2016.7.16
40	132.9958	35.4465	4.9	2016.7.16
41	132.9551	35.4459	5.6	2016.7.16
<b>Nakaumi -</b>				
N1	133.1468	35.4597	4.5	2016.7.31
N2	133.1700	35.4637	6.1	2016.7.31
N3	133.1878	35.4654	6.5	2016.7.31
N4	133.2145	35.4591	6.3	2016.7.31
N5	133.2083	35.4644	6.7	2016.7.31
N6	133.2016	35.4692	6.7	2016.12.17
N7	133.1963	35.4752	6.8	2016.12.17

Comparison of different radionuclide dating models for estimating the ages of  
sediments from Lakes Shinji-ko and Nakaumi, Japan

**Appendix 2** Sediment age estimates for the models used for site Shinji-ko-15. Shaded rows indicate the 14.0–14.5 cm core section with the <sup>137</sup>Cs 1963 time marker. \* indicates the results obtained with the Excel application by Sanchez-Cabeza and Ruiz-Fernández (2012). CIC: Constant Initial Concentration, CFCS: Constant Flux Constant Sedimentation, CRS: Constant Rate of Supply, SIT: Sediment Isotope Tomography, TERESA: Time Estimates from Random Entries of Sediments and Activities, CA: Constant Activity, CF: Constant Flux.

Shinji-ko-15	(1)	(2)	(2')	(3)	(4)	(5)	(6)	(7)	(8)						
Core Depth (cm)	Mass Depth	CIC (age)	±	CFCS (age) piecewise	±	CFCS (age) non-piecewise	±	CRS (age)	±	Composite CRS (age)	±	SIT (age)	TERESA (age)	CA * (age)	CF* (age)
0.25	0.09	2.0	0.9	1.2	0.9	0.8	0.9	0.5	0.0	0.6	0.0	0.9	0.9	2.1	
0.50															1.1
0.75	0.17	2.1	1.0	2.4	1.0	1.5	1.0	1.5	0.1	1.7	0.1	2.7	1.8	2.2	
1.00															2.1
1.25	0.25	3.1	1.0	3.6	1.0	2.3	1.0	2.5	0.1	2.9	0.2	4.4	3.5	3.1	
1.50															3.2
1.75	0.34	5.6	1.0	4.8	1.0	3.1	1.0	3.5	0.1	4.0	0.2	6.2	4.6	5.7	
2.00															4.3
2.25	0.43	6.8	1.4	6.2	1.4	4.0	1.4	4.7	0.2	5.3	0.2	8.0	5.8	6.9	
2.50															5.1
2.75	0.53	10.3	1.0	7.5	1.0	4.9	1.0	5.8	0.2	6.6	0.3	9.7	6.7	10.4	
3.00															6.2
3.25	0.63	10.3	1.2	9.0	1.2	5.9	1.2	6.9	0.2	7.9	0.3	11.5	7.5	10.4	
3.50															7.3
3.75	0.73	8.8	1.0	10.4	1.0	6.8	1.0	8.1	0.2	9.3	0.3	13.3	9.3	8.9	
4.00															8.6
4.25	0.84	11.5	1.1	12.0	1.1	7.8	1.1	9.4	0.2	10.8	0.4	15.1	10.8	11.6	
4.50															9.7
4.75	0.95	13.3	1.0	13.5	1.0	8.8	1.0	10.6	0.3	12.3	0.4	16.8	12.1	13.4	
5.00															11.0
5.25	1.07	15.3	1.2	15.3	1.2	10.0	1.2	12.0	0.3	14.0	0.4	18.6	13.1	15.4	
5.50															12.6
5.75	1.19	19.7	1.1	17.0	1.1	11.1	1.1	13.4	0.3	15.5	0.5	20.4	14.3	19.8	
6.00															13.9
6.25	1.32	18.7	1.0	18.8	1.0	12.3	1.0	14.7	0.3	17.2	0.5	22.1	16.1	18.8	
6.50															15.3
6.75	1.45	24.8	1.1	20.8	1.0	13.6	1.0	16.1	0.3	18.9	0.5	23.9	17.3	24.9	
7.00															16.7
7.25	1.60	23.8	1.1	22.8	1.1	14.9	1.1	17.5	0.4	20.7	0.6	25.7	19.0	23.9	
7.50															18.2
7.75	1.74	25.7	1.0	24.9	1.0	16.3	1.0	19.0	0.4	22.5	0.6	27.5	20.3	25.9	
8.00															19.7
8.25	1.88	25.9	1.2	26.9	1.2	17.6	1.2	20.5	0.4	24.3	0.7	29.2	22.2	26.1	
8.50															21.1
8.75	2.03	31.8	1.1	29.0	1.1	19.0	1.1	22.0	0.4	26.2	0.7	31.0	24.6	32.0	
9.00															22.5
9.25	2.19	35.0	1.4	31.3	1.4	20.5	1.4	23.4	0.4	28.1	0.8	32.8	28.4	35.1	
9.50															24.1
9.75	2.34	28.8	1.3	33.4	1.3	21.8	1.3	24.8	0.5	30.0	0.8	34.5	31.2	28.9	
10.00															25.7
10.25	2.50	35.5	1.2	35.0	1.2	23.4	1.2	26.6	0.5	32.3	0.9	36.3	32.5	35.7	
10.50															27.7
10.75	2.66	38.2	1.5	36.6	1.5	24.9	1.5	28.1	0.5	34.4	1.0	38.1	35.0	38.3	
11.00															29.6
11.25	2.83	39.6	1.5	38.3	1.5	26.4	1.5	29.6	0.5	36.4	1.1	39.9	37.0	39.7	
11.50															31.3
11.75	2.99	39.7	1.3	40.0	1.3	28.0	1.3	31.1	0.6	38.6	1.2	41.6	38.5	39.8	
12.00															32.8
12.25	3.17	43.0	1.7	41.7	1.7	29.6	1.7	32.7	0.6	40.9	1.3	43.4	40.4	43.2	
12.50															34.6
12.75	3.33	41.7	1.6	43.4	1.6	31.2	1.6	34.3	0.6	43.3	1.6	45.2	42.9	41.9	
13.00															36.2
13.25	3.51	46.6	1.4	45.2	1.4	32.8	1.4	36.0	0.6	45.8	1.9	46.9	44.9	46.8	
13.50															37.7
13.75	3.67	43.6	1.4	46.8	1.4	34.3	1.4	37.6	0.7	48.2	2.7	48.7	46.2	43.7	
14.00															39.5
14.25	3.85	54.7	2.1	48.6	2.1	36.0	2.1	39.2	0.7	50.8		50.5	48.0	54.9	
14.50															41.2
14.75	4.03	48.7	1.5	50.4	1.6	37.6	1.6	40.8	0.7	54.0	0.3	52.3	51.0	48.9	
15.00															43.1
15.25	4.22	53.1	2.2	52.3	2.2	39.4	2.2	42.5	0.8	55.8	0.3	54.0	53.6	53.4	
15.50															45.0
15.75	4.42	55.1	2.2	54.3	2.2	41.3	2.2	44.3	0.8	57.6	0.4	55.8	55.8	55.3	

## Appendix 2 Continued.

16.00															46.9
16.25	4.61	58.3	2.8	56.3	2.8	43.1	2.8	46.1	0.9	59.3	0.4	57.6	58.2	58.5	
16.50															48.5
16.75	4.81	60.7	2.5	58.3	2.5	45.0	2.5	47.7	0.9	61.0	0.5	59.3	61.4	60.9	
17.00															50.4
17.25	5.01	62.6	2.1	60.4	2.1	46.9	2.1	49.4	0.9	62.7	0.5	61.1	64.0	62.9	
17.50															52.0
17.75	5.21	57.8	1.9	62.4	1.9	48.7	1.9	51.3	1.0	64.5	0.6	62.9	66.1	58.0	
18.00															53.8
18.25	5.42	62.9	2.7	64.5	2.7	50.7	2.7	53.3	1.0	66.6	0.6	64.6	68.7	63.2	
18.50															55.7
18.75	5.64	69.8	2.5	66.7	2.5	52.7	2.5	55.2	1.1	68.4	0.7	66.4	71.2	70.1	
19.00															57.4
19.25	5.86	66.0	3.0	68.0	3.0	54.7	3.0	57.1	1.2	70.3	0.8	68.2	73.4	66.2	
19.50															59.6
19.75	6.08	67.8	2.4	69.5	2.5	56.8	2.5	59.2	1.2	72.5	0.8	69.9	77.7	68.1	
20.00															61.8
20.50	6.53	63.4	2.9	72.4	2.9	61.0	2.9	64.2	1.4	77.5	1.0	72.6	84.6	63.6	
21.00															68.2
21.50	7.01	73.9	3.7	75.5	3.7	65.6	3.7	70.1	1.6	83.4	1.3	76.1	91.0	74.2	
22.00															74.2
22.50	7.52	73.8	3.7	78.7	3.7	70.3	3.7	76.2	1.8	89.5	1.5	79.7	96.4	74.1	
23.00															80.7
23.50	8.03	80.5	3.5	82.0	3.5	75.0	3.5	83.2	2.0	96.5	1.8	83.2	105.2	80.8	
24.00															86.8
24.50	8.54	81.2	4.5	85.2	4.5	79.8	4.5	90.9	2.4	104.2	2.2	86.7	110.6	81.5	
25.00															94.7
25.50	9.06	80.6	3.3	91.6	3.3	84.7	3.3	101.5	2.9	114.8	2.6	90.3	125.4	80.9	
26.00															105.4
26.50	9.60	95.5	4.6	98.0	4.6	89.7	4.6	114.0	3.6	127.4	3.5	93.8	137.3	95.9	
27.00															115.0
27.50	10.15	95.6	4.6	104.7	4.7	94.9	4.7	129.5	5.1	142.9	4.9	97.4	145.4	96.0	
28.00															132.9
28.50	10.70	104.0	8.3	111.3	8.3	100.0	8.3	155.1	9.0	168.5	8.8	100.9	168.1	104.4	
29.00															156.3
29.50	11.27	109.7	9.1	118.2	9.1	105.4	9.1					104.4	173.4	110.1	

Comparison of different radionuclide dating models for estimating the ages of  
sediments from Lakes Shinji-ko and Nakaumi, Japan

**Appendix 3** Sediment age estimates for the models used for site Nakaumi-N3. Shaded rows indicate the 7.5–8.5 cm core section with the <sup>137</sup>Cs 1963 time marker. \* indicates the results obtained with the Excel application by Sanchez-Cabeza and Ruiz-Fernández (2012). CIC: Constant Initial Concentration, CFCS: Constant Flux Constant Sedimentation, CRS: Constant Rate of Supply, SIT: Sediment Isotope Tomography, TERESA: Time Estimates from Random Entries of Sediments and Activities, CA: Constant Activity, CF: Constant Flux.

Nakaumi-N3		(1)	(2)	(2')	(3)	(4)	(5)	(6)	(7)	(8)					
Core Depth (cm)	Mass Depth	CIC (age)	±	CFCS (age) piecewise	±	CFCS (age) non-piecewise	±	CRS (age)	±	Composite CRS (age)	±	SIT (age)	TERESA (age)	CA * (age)	CF* (age)
0.25	0.25	19.3	1.3					1.5	0.0	1.9	0.1	1.6	1.9	15.4	
0.50	0.32														1.8
0.75	0.38	21.0	1.4					3.2	0.2	3.8	0.4	4.9	5.8	17.5	
1.00	0.45														3.1
1.25	0.52	19.2	1.0					5.0	0.3	6.0	0.4	8.2	8.1	15.4	
1.50	0.59														5.9
1.75	0.67	20.1	1.1					7.1	0.3	8.6	0.5	11.5	11.2	16.5	
2.00	0.74														8.1
2.25	0.82	18.0	1.2	17.0	1.2	7.8	1.3	9.4	0.4	11.6	0.6	14.8	14.6	14.4	
2.50	0.89														10.3
2.75	0.97	25.8	1.0	20.2	1.0	9.5	1.3	11.8	0.4	14.7	0.7	18.1	16.8	22.4	
3.00	1.05														13.2
3.25	1.13	23.3	1.3	23.5	1.3	11.2	1.0	14.1	0.4	17.8	0.7	21.3	18.9	19.5	
3.50	1.21														15.5
3.75	1.28	26.0	1.4	26.7	1.4	13.0	1.1	16.7	0.5	21.3	0.8	24.6	20.8	22.8	
4.00	1.36														18.0
4.25	1.44	30.3	1.4	30.1	1.4	14.8	1.2	19.3	0.5	24.8	0.9	27.8	24.0	26.9	
4.50	1.53														19.8
4.75	1.61	38.1	1.6	33.5	1.6	16.6	1.0	21.6	0.5	28.2	1.0	31.1	29.1	35.4	
5.00	1.69														23.2
5.25	1.77	37.2	1.9	36.9	1.9	18.5	1.3	23.8	0.6	31.5	1.1	34.3	32.3	34.5	
5.50	1.85														25.1
5.75	1.93	45.5	1.5	40.3	1.5	20.3	1.4	26.0	0.6	34.8	1.2	37.5	35.3	43.6	
6.00	2.02														27.4
6.25	2.10	44.8	1.8	43.7	1.8	22.2	1.4	28.0	0.6	38.1	1.4	40.6	37.7	43.0	
6.50	2.18														29.7
6.75	2.27	52.1	1.7	47.3	1.7	24.1	1.6	30.1	0.7	41.5	1.6	43.8	46.7	51.0	
7.00	2.35														31.7
7.25	2.44	50.1	1.6	50.8	1.6	26.0	1.9	32.0	0.7	45.0	2.0	46.9	49.5	49.1	
7.50	2.53														34.4
7.75	2.61	48.6	1.9	52.8	1.9	28.0	1.5	34.3	0.7	49.2	3.0	50.1	52.1	47.5	
8.00	2.70														36.8
8.25	2.79	53.3	1.8	54.7	1.8	30.0	1.8	36.7	0.8	53.9		53.2	55.0	51.9	
8.50	2.88														39.4
8.75	2.97	53.9	2.2	56.7	2.2	32.0	1.7	39.2	0.8	56.3	0.3	56.2	57.4	53.3	
9.00	3.06														42.4
9.25	3.15	56.5	2.3	58.8	2.3	34.0	1.6	41.7	0.8	58.8	0.4	59.3	59.3	55.8	
9.50	3.24														45.5
9.75	3.34	57.8	1.9	60.8	1.9	36.1	1.9	44.2	0.9	61.4	0.5	62.3	66.0	57.8	
10.00	3.43														49.0
10.25	3.52	60.1	2.0	62.8	2.0	38.1	1.8	46.8	0.9	64.0	0.6	65.3	70.0	60.4	
10.50	3.61														51.6
10.75	3.70	61.6	2.2	64.9	2.2	40.2	2.2	49.5	1.0	66.7	0.6	68.3	73.3	62.3	
11.00	3.80														55.0
11.25	3.89	67.7	3.1	66.4	3.1	42.3	2.3	52.2	1.0	69.4	0.7	71.3	76.3	70.0	
11.50	3.99														58.1
11.75	4.09	68.3	2.5	68.1	2.5	44.6	1.9	55.0	1.1	72.2	0.8	74.2	81.0	70.8	
12.00	4.19														61.6
12.25	4.29	71.7	2.7	69.6	2.7	46.8	2.0	57.8	1.2	75.0	0.9	77.1	83.2	74.1	
12.50	4.39														64.7
12.75	4.48	71.4	2.7	71.2	2.7	49.0	2.1	60.7	1.3	77.9	0.9	80.0	86.6	73.6	
13.00	4.58														68.5
13.25	4.69	75.7	3.8	72.9	3.8	51.2	3.1	63.8	1.3	81.0	1.0	82.9	89.2	80.7	
13.50	4.78														72.1
13.75	4.88	75.5	3.9	74.5	3.9	53.5	2.5	67.0	1.4	84.2	1.1	85.8	91.9	80.2	
14.00	4.99														76.4
14.25	5.09	76.6	3.0	76.1	3.0	55.7	2.7	70.5	1.5	87.7	1.3	88.6	96.9	82.5	
14.50	5.22														81.0
14.75	5.35	70.2	3.8	79.5	3.8	58.7	2.7	76.3	1.8	93.5	1.5	91.4	101.1	73.1	

## Appendix 3 Continued.

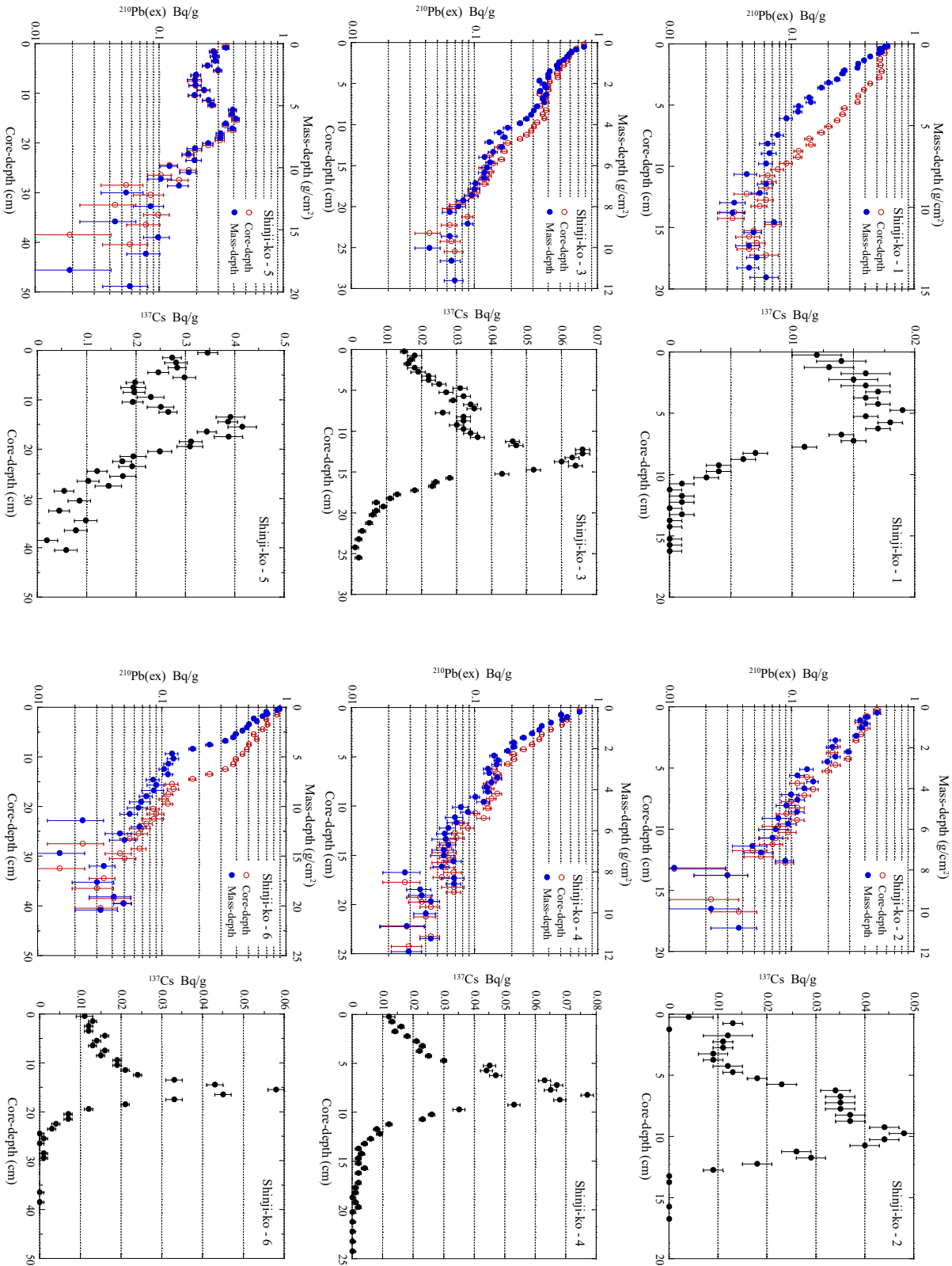
15.00	5.45														89.4
15.25	5.55	76.8	3.1	82.1	3.1	61.0	3.8	81.5	1.8	98.7	1.6	94.3	105.4	81.7	
15.50	5.65														97.0
15.75	5.76	81.0	3.5	84.7	3.5	63.3	3.9	86.8	2.0	104.0	1.8	97.0	109.5	87.6	
16.00	5.86														104.3
16.25	5.96	85.4	6.2	87.3	6.2	65.6	3.0	92.3	2.3	109.5	2.1	99.8	113.2	98.4	
16.50	6.07														110.9
16.75	6.18	84.2	3.6	90.1	3.6	68.0	3.8	98.8	2.5	116.0	2.3	102.6	115.9	93.1	
17.00	6.28														119.6
17.25	6.39	93.9	4.9	92.8	4.9	70.4	3.1	105.8	2.8	123.1	2.7	105.3	121.3	118.2	
17.50	6.49														125.4
17.75	6.60	88.4	6.5	95.5	6.5	72.7	3.5	114.1	3.4	131.3	3.2	108.1	123.9	105.0	
18.00	6.70														135.5
18.25	6.80	92.8	4.5	98.1	4.5	75.0	6.2	125.1	3.7	142.4	3.6	110.8	127.2	107.5	
18.50	6.91														149.6
18.75	7.01	99.1	8.1	100.7	8.1	77.3	3.6	138.8	4.9	156.1	4.8	113.5	131.1	131.1	
19.00	7.11														160.4
19.25	7.21	95.7	5.2	103.3	5.2	79.6	4.9	160.8	5.8	178.1	5.7	116.3	136.5	116.7	
19.50	7.31														186.7
19.75	7.41	99.3	6.1	105.9	6.1	81.9	6.5					119.0	139.5	126.6	

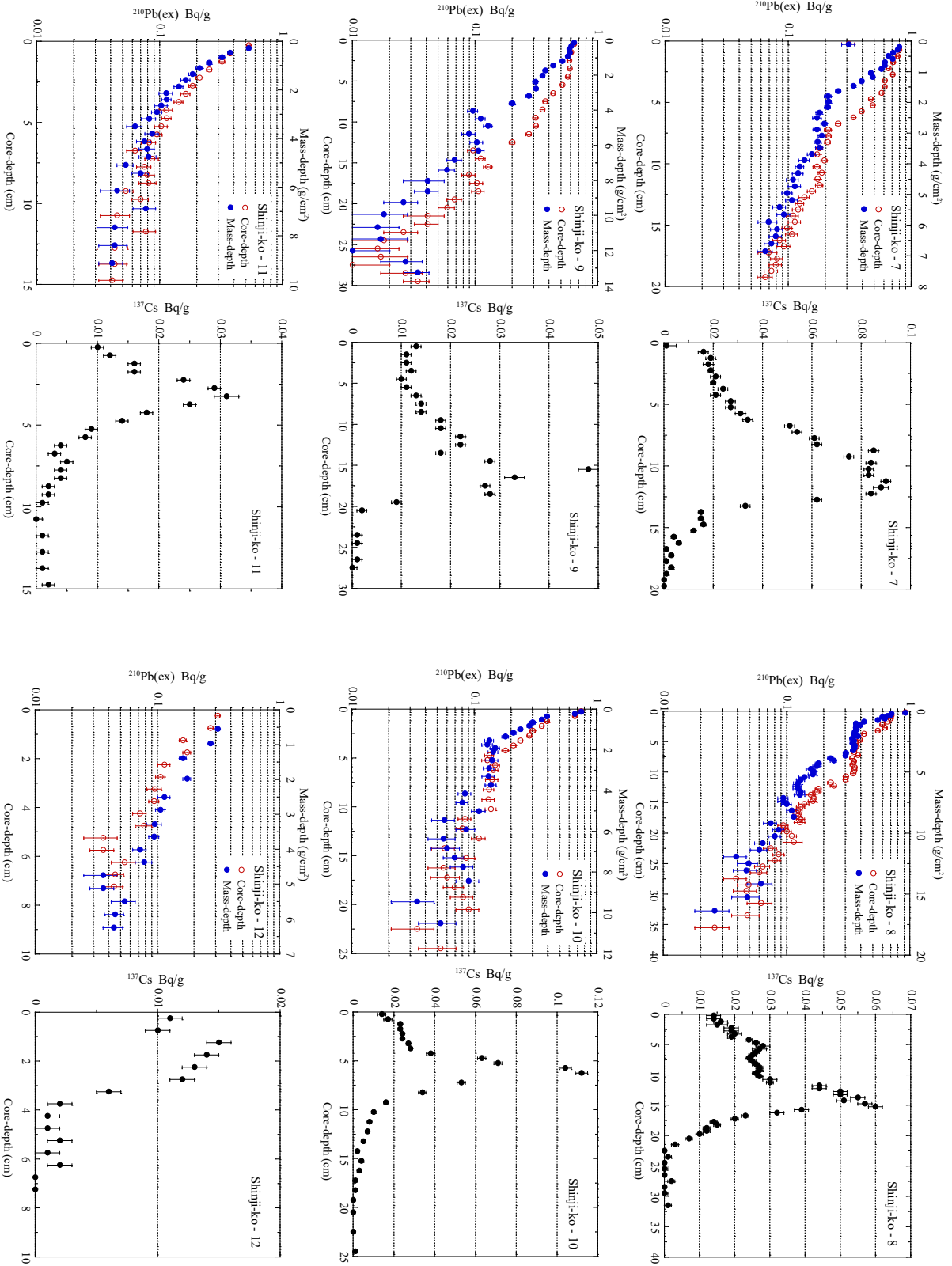
Appendix 4-11 Depth distributions of  $^{210}\text{Pb}_{\text{ex}}$  and  $^{137}\text{Cs}$  at sites Shinji-ko-1-41 and Nakaumi-N1-N



Comparison of different radionuclide dating models for estimating the ages of sediments from Lakes Shinji-ko and Nakaumi, Japan

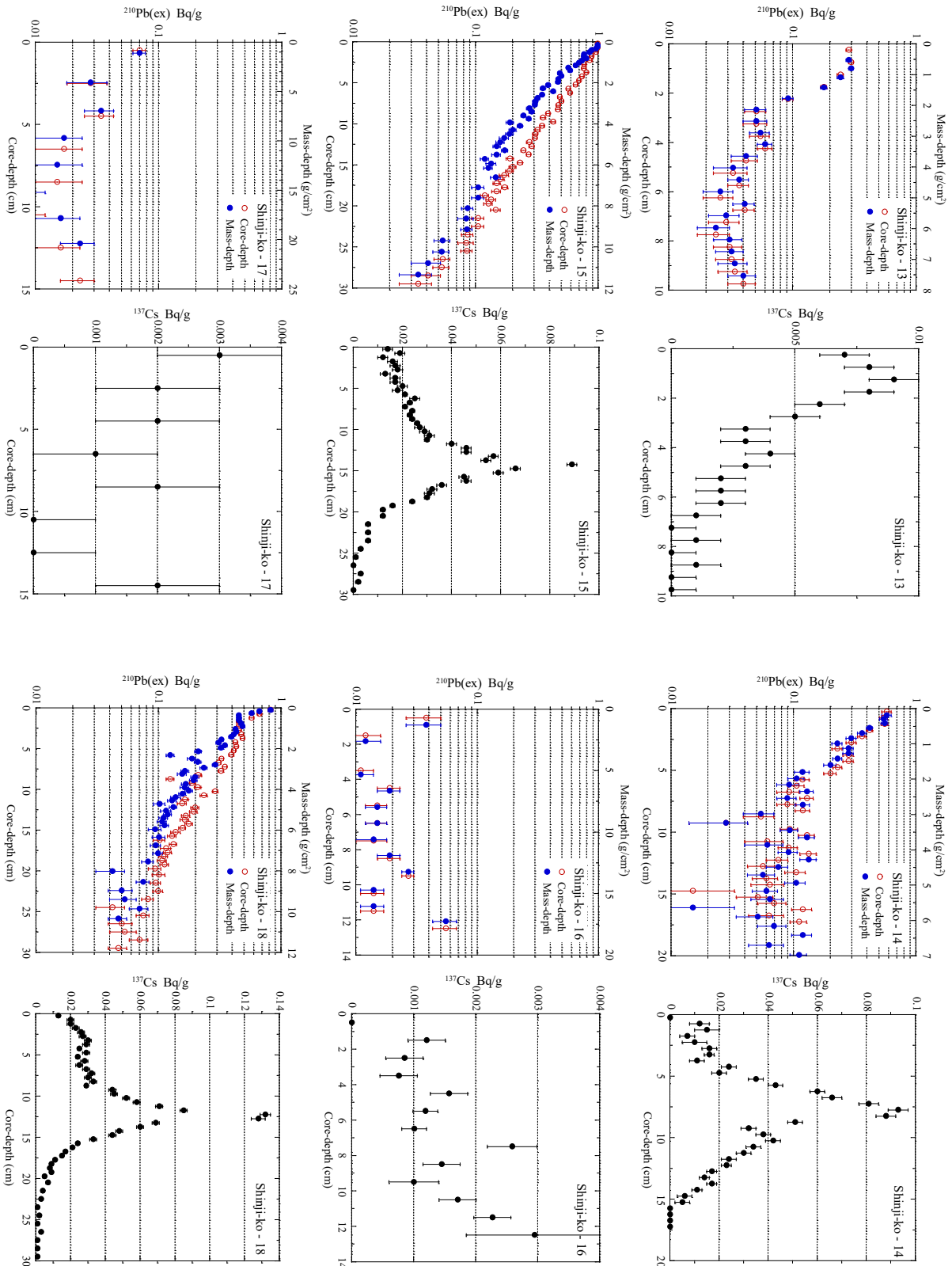
Appendix 4

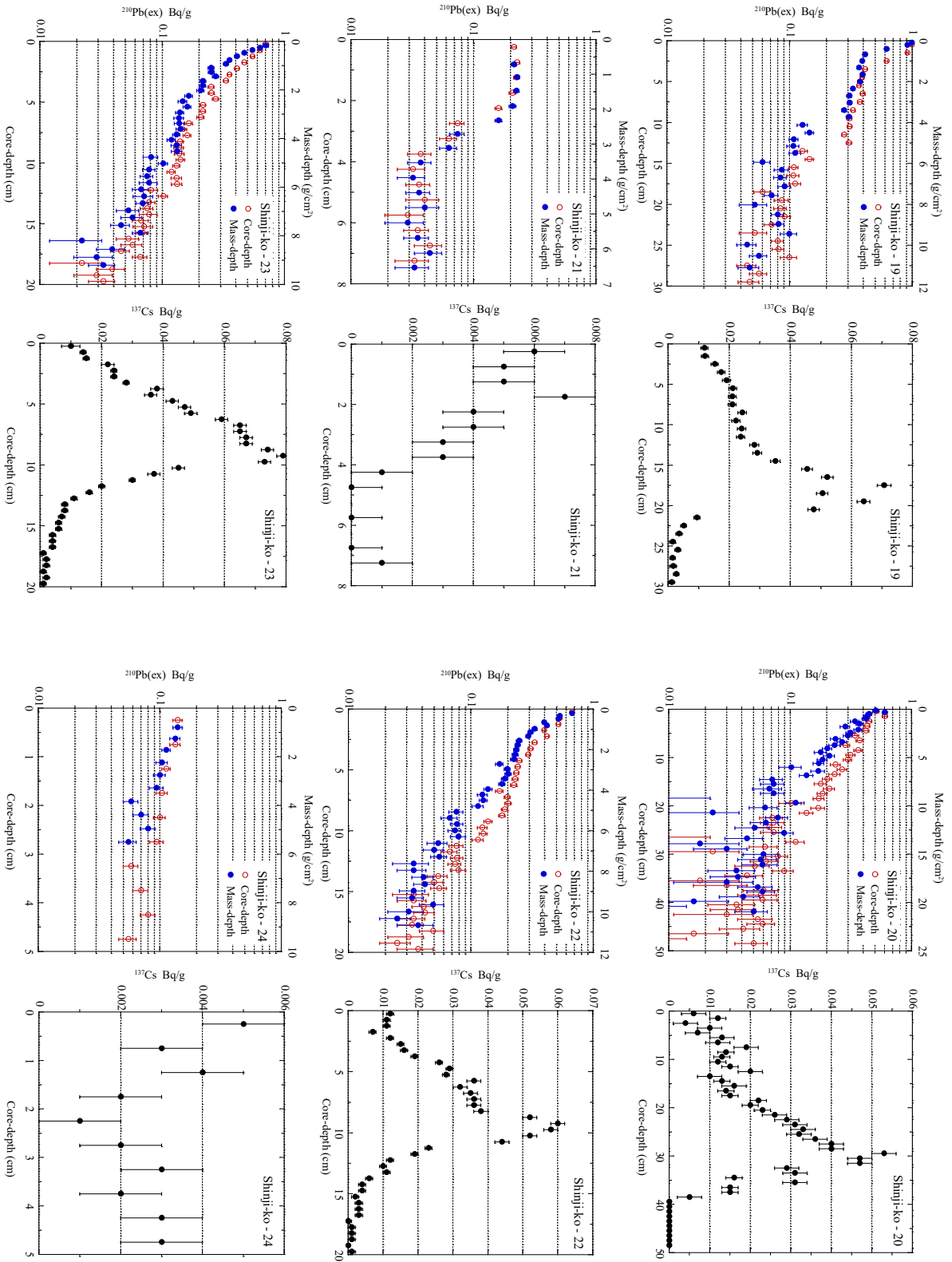




Comparison of different radionuclide dating models for estimating the ages of sediments from Lakes Shinji-ko and Nakaumi, Japan

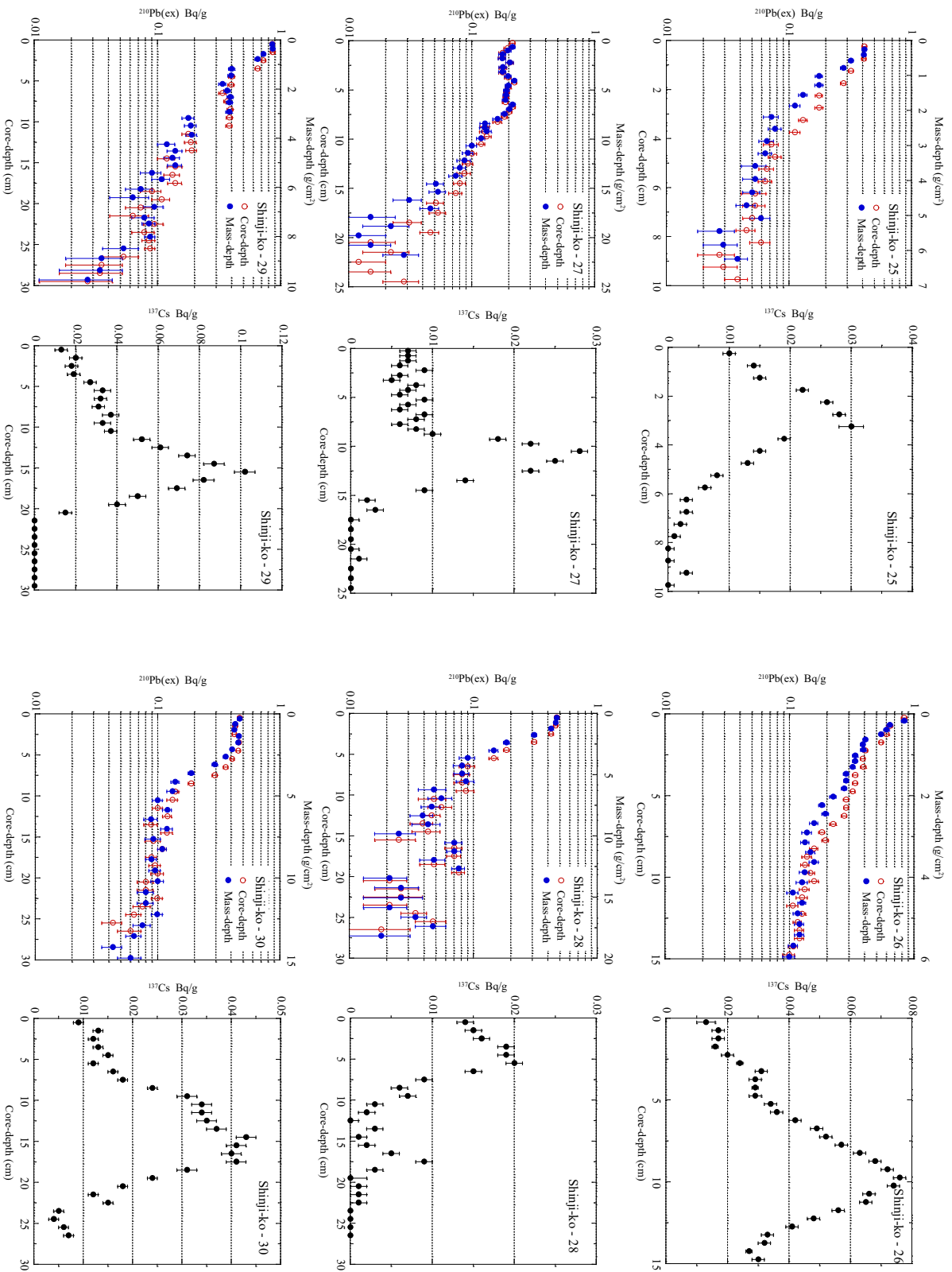
Appendix 6

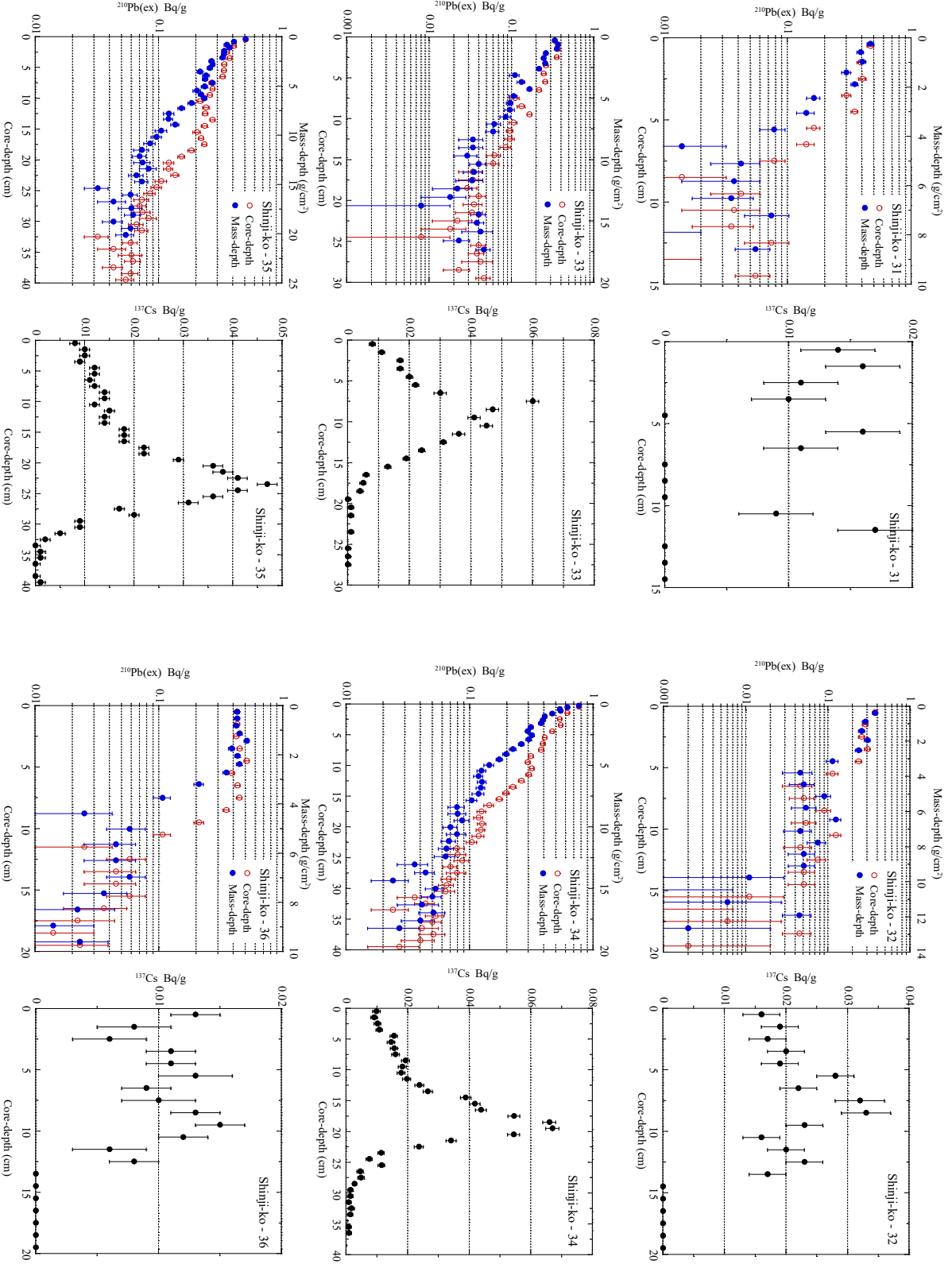




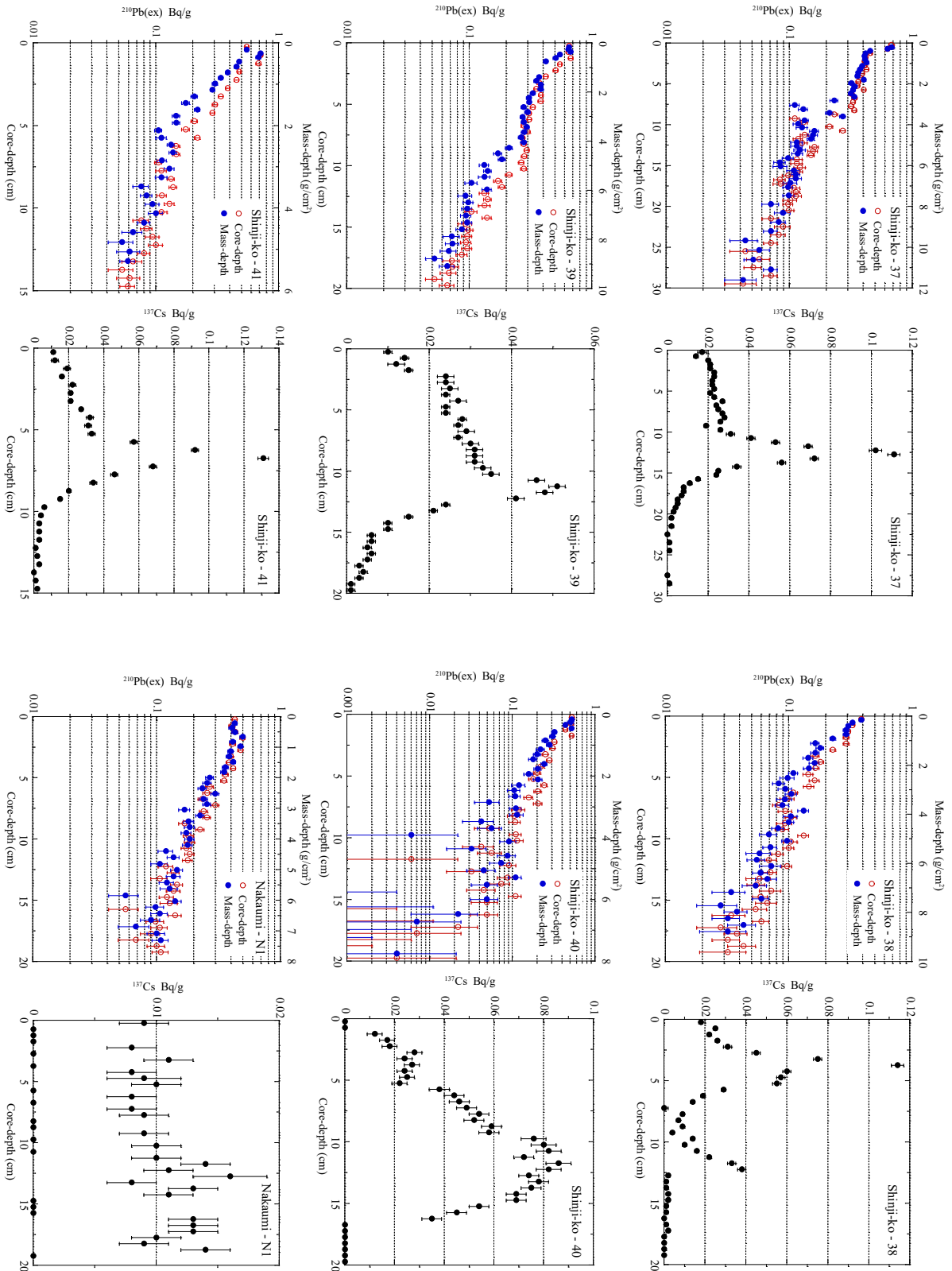
Comparison of different radionuclide dating models for estimating the ages of sediments from Lakes Shinji-ko and Nakaumi, Japan

Appendix 8





Comparison of different radionuclide dating models for estimating the ages of sediments from Lakes Shinji-ko and Nakaumi, Japan



Appendix 11

